Jour. Petrol. Soc. Korea
Vol. 8, No. 1, p. 46~55, 1999

A Fluid inclusion study of the Sannae granite and the associated Sannae W-Mo deposit, Southeastern Kyongsang Basin

Kyounghee Yang and Joon Dong Lee

Department of Geology, Pusan National University, Pusan 609-735, Korea

ABSTRACT : Fluid inclusions in granite and hydrothermal quartz indicate that three fluids have affected the Sannae granite. The earliest fluid is represented by three-phase aqueous fluid inclusions with high salinity (38 to 46 wt.% NaCl equiv.). It was exsolved from a crystallizing melt and trapped at a relatively high-pressure condition. The second fluid is represented by two-phase aqueous fluid inclusions with low eutectic temperatures (<-40℃), low- to moderate- salinity (3 to 24.0 wt.% NaCl equiv.) and high homogenization temperatures (309℃<Th_{L-V}<473℃). This fluid was trapped at higher pressures than 300-500 bars and precipitated molybdenite and wolframite in quartz veins. It was probably generated by fluid-host rock interactions since they show a wide range of salinity within a narrow range of homogenization temperatures. The final fluid is represented by an aqueous fluid boiling that separated into high-salinity (34-38 wt.% NaCl equiv.) and low-salinity fluid (0 to 8.7 wt.%) at 303-376℃ and 50-150 bars. These boiling fluids precipitated euhedral quartz in miarolitic cavities. The compositions of the final fluid was rather complex in the H_2O-NaCl-KCl-$FeCl_2$ system. The Sannae granite was a locus for repeated fluid events including magmatic fluids during the final stage of crystallization, the convection of hydrothermal fluids causing a fluid ascending, fluid boiling, and the local W-Mo mineralization and formation of miarolitic cavities due to thermal, tectonic and compositional properties of the felsic granite.

Key words : fluid inclusion, hydrothermal quartz, exsolution, aqueous fluid immiscibility, W-Mo mineralization

INTRODUCTION

The hydrothermal vein-type deposit of the Sannae W-Mo mine is developed within the Cretaceous-early Tertiary granite (referred to locally as the Sannae granite) of the Kyongsang Basin in the southeastern part of the Korean peninsula (Fig. 1). The granitic rocks hosting the Sannae W-Mo mine show a diversity in color, texture and mineralogy suggesting shallow-seated intrusives (Bajwah *et al.*, 1995). In addition, abundant miarolitic cavities in the granitic rocks indicate the presence of fluids during late-stage crystallization of the granite. Shallow-seated plutons generally form thermal anomalies which are predicted to cause fluid convection. This provides an explanation for the widespread alteration, veining and mineralization which are commonly observed in granites of the Kyongsang Basin (e. g. Yang and Lee, 1998; Yang, 1996a, b). The granitic rocks at the Sannae mining district experienced the intensive hydrothermal activities evidenced by fissure-filling veins cemented by W-Mo ore minerals and quartz, the pervasive alteration of host granitic rocks and the occurrence of euhedral quartz in the miarolitic cavities.

Shelton *et al.* (1986) carried out geologic, isotopic and fluid inclusion studies on the Sannae Mo-W mine, focussing only on the vein mineralization. The present study is focused on the fluid inclusion in magmatic and hydrothermal

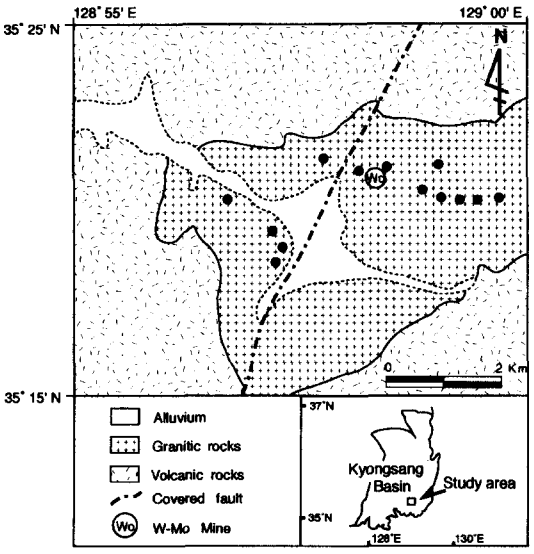

Fig. 1. Geologic map of the Sannae mine area (after Hong and Choi, 1988). Solid circles are sample localities.

quartz and presents data on the temperature, pressure, and compositions of fluids as well as the evolution of fluid properties in the magmatic-hydrothermal system in relation to the Sannae granite.

GENERAL GEOLOGY AND THE SANNAE ORE DEPOSIT

The Sannae granitic rocks containing the W-Mo ore mineralization intrude Cretaceous sedimentary and volcanic rocks of the Basin (Fig. 1). The fabric of the pluton is massive. There is no tendency for minerals to be oriented either as lineation or foliation. It is classified as a biotite-granite (Hong and Choi, 1988) containing abundant miarolitic cavities. Some miarolitic cavities hosts big and euhedral quartz crystals throughout the whole pluton. Schlieren composed of mafic minerals are found where subangular to ellipsoidal country rock xenoliths are common. Well-developed sheet joints are also common.

The granitic rocks are composed of medium to fine, anhedral to subhedral quartz, K-feldspar, plagioclase, biotite and rarely zircon. The biggest phenocrysts are plagioclase although they are not as abundant as quartz phenocrysts. Plagioclase phenocrysts often show zonal textures and the central part of the zoned plagioclase is shattered and altered to sericite. Albite rimming the K-feldspar has been observed. Quartz phenocrysts are highly corroded, microfractured and broken into three or four parts showing resorbed boundaries. Quartz is also interstitial to K feldspar and plagioclase. Relatively big K-feldspar is perthitic and is altered with sericite. Biotite is the dominant mafic mineral and occurs either as large crystals or as fine platy crystals with irregular grain boundaries disseminated in the matrix. Hornblende is rarely observed. Accessory minerals are zircon, apatite, sphene and magnetite.

The granitic rocks containing the fissure-filling quartz veins grade into sericite-dominated rocks toward the vein margin. Alteration processes affecting the wall rock are probably related to the formation of the veins. The alteration minerals are of sericite, epidote, and chlorite. Sericite occurs as fine aggregates which are irregularly distributed in the matrix or within feldspars. Quartz occurs as secondary mosaics produced during hydrothermal alteration along the vein margin.

A large number of subparallel fissure-filling quartz veins are associated with molybdenite-tungsten mineralization. The ore minerals of the fissure-filling quartz veins mainly include molybdenite, wolframite and scheelite (Shelton *et al.*, 1986). According to Shelton *et al.* (1986), the mineral paragenesis is simple and can be divided into three stages: early molybdenum stage, main tungsten stage, and late carbonate stage. Quartz was deposited through all stages. In the early molybdenum stage, milky fine-grained anhedral quartz and molybdenite was precipitated. During the late molybdenum stage, the deposition of prismatic, euhedral milky or clear quartz with wolframite and scheelite occurred. Clear quartz and calcite were then deposited in the remaining open space. Carbonate mineralization stage occurs as vug-filling. More detailed descriptions for the mineral paragene-

sis are shown in Shelton *et al.* (1986).

FLUID INCLUSIONS

Petrography

Hydrothermal quartz in molybdenite- and wolframite-bearing fissure-filling veins, euhedral quartz in miarolitic cavities and magmatic quartz in granitic rocks were collected for this study. Doubly-polished plates varying in thickness between 0.07 to 0.1 mm were prepared for petrographic and microthermometric analysis in order to determine the fluid compositions and trapping temperatures of fluid inclusions. Based on the criteria of Roedder (1984), fluids are regarded to have been trapped as primary, pseudosecondary, and secondary inclusions. Many secondary inclusions occur along microfractures in quartz veins, but the time relationships between different generations of secondary inclusions could not be established. Thus, only primary inclusions were examined in this study.

Three types of fluid inclusions were identified based on the phase behavior at room temperature (Fig. 2). Type I inclusions are aqueous vapor-rich with a vapor bubble occupying greater than 80 vol % of the inclusions (Fig. 2a). They occur in quartz from miarolitic cavities and are characterized by low salinity. Type II inclusions are aqueous liquid-rich with a vapor bubble occupying less than 40 vol% of the inclusion (Fig. 2b). They occur in fissure-filling hydrothermal quartz vein and are characterized by low to moderate salinity. Type III inclusions are aqueous liquid-rich containing halite with or without other daughter crystals (Fig. 2c and d). They occur in both magmatic and hydrothermal quartz and are characterized by high salinity.

Quartz from granitic rocks

Primary type IIIa inclusions in granitic rocks occur as isolated inclusions. Quartz phenocrysts are cloudy and highly embayed, and also contain crystallized melt inclusions and secondary types I and II inclusions. Type III inclusions contain halite, a vapor bubble, and sometimes a birefringent crystal and opaque crystals, indicating dense brines (Fig. 2c). This type of inclusions show fairly consistent phase ratios and form a single, discrete population.

Quartz from hydrothermal veins

Quartz from fissure-filling veins varies in

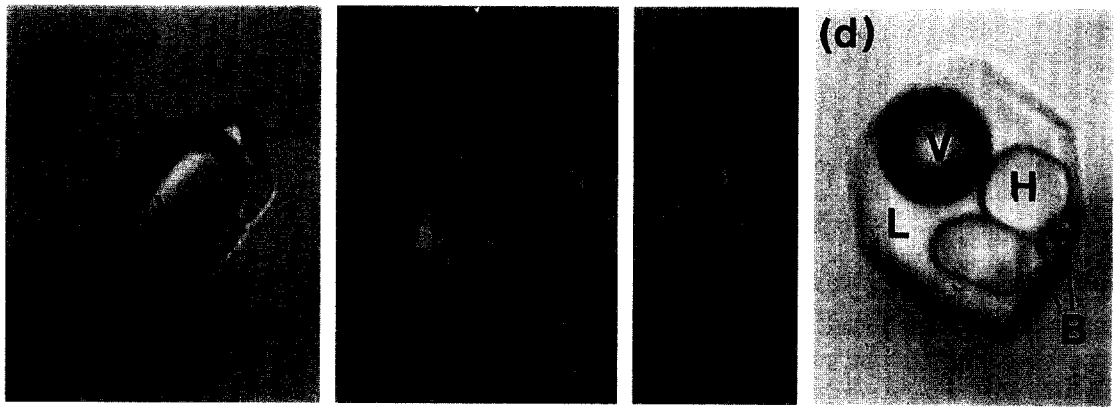

Fig. 2. Photomicrographs of different types of fluid inclusions observed in the Sannae granite area. (a) Type I vapor-rich inclusions (100 μm) in quartz from a miarolitic cavity. (b) Type II liquid-rich inclusions (20 μm) in quartz vein. (c) Type IIIa halite-bearing inclusions (10 μm) in magmatic quartz. Note relatively large halite crystal and a small vapor bubble. (d) Type IIIb halite-bearing inclusions (120 μm) in quartz from a miarolitic cavity. L=liquid, V=vapor bubble, H=halite, B=unidentified birefringent crystal.

color from milky quartz (at the crystal base) to clear (at the crystal terminations) and contains primary type II inclusions (Fig. 2b). They are distributed randomly or occur along growth zones and have consistent phase ratios. They have a relatively large vapor bubble, implying the low density of the fluid and/or a high-temperature fluid. Although type I inclusions without a liquid phase are present in the examined samples, the origin of the vapor-rich type I inclusions is ambiguous. No visible liquid phase in type I inclusions indicates a low-temperature trapping.

Quartz from miarolitic cavities

Most type I (Fig. 2a) and III inclusions (Fig. 2d) occur together along well-defined growth zones of euhedral miarolitic quartz indicating almost certain boiling conditions. Type I inclusions sometimes contain an opaque solid phase (Fig. 2a). Type III inclusions (Fig. 2d) contain halite and sylvite, one or two birefringent daughter crystals, and one or two opaque grains. The birefringent grains with somewhat rectangular crystal forms are thought to be erythrosiderite ($K_2FeCl_5 \cdot H_2O$) based on the color, refractive index and strong birefringence (e. g., Stefanini and Williams-Jones, 1996; Yang and Lee, 1998). Type II are not present as primary inclusions in euhedral quartz from miarolitic cavities.

MICROTHERMOMETRY

Heating and cooling experiments were carried out using a Linkam Th 600 heating and freezing stage. The stage was calibrated with pure CO_2 and pure H_2O synthetic fluid inclusions (Bodnar and Sterner, 1987). The accuracy and reproducibility of temperatures of phase changes are approximately ±0.1℃ at T≤ 50℃; ±0.5℃ at T≤374.1℃; and ±5℃ at T≤ 573℃. Microthermometric measurements were made to obtain homogenization temperature (Th) and compositions (Fig. 3 and 4). Salinities of aqueous inclusions were calculated using the program SALTY of Bodnar *et al.* (1989) and Bodnar and Vityk (1994). Although fluid inclusions seemed to be one group of generation, the inclusions with inconsistent homogenization temperatures were excluded from the study.

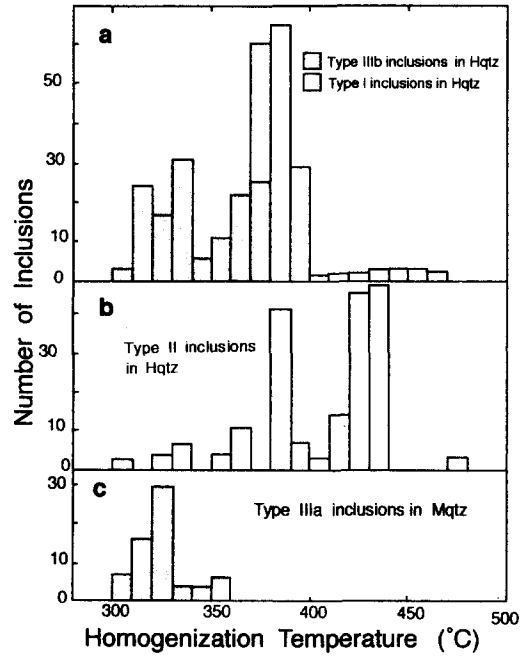

Fig. 3. Frequency histogram of homogenization temperatures of fluid inclusions. Mqtz=magmatic quartz, Hqtz=hydrothermal quartz.

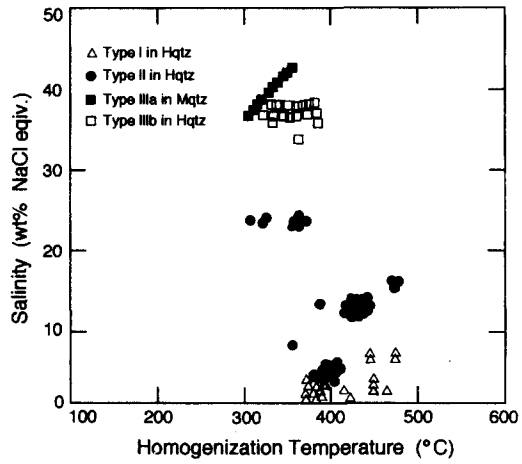

Fig. 4. Homogenization temperatures of fluid inclusions plotted against salinities. For abbreviations, see Fig. 3.

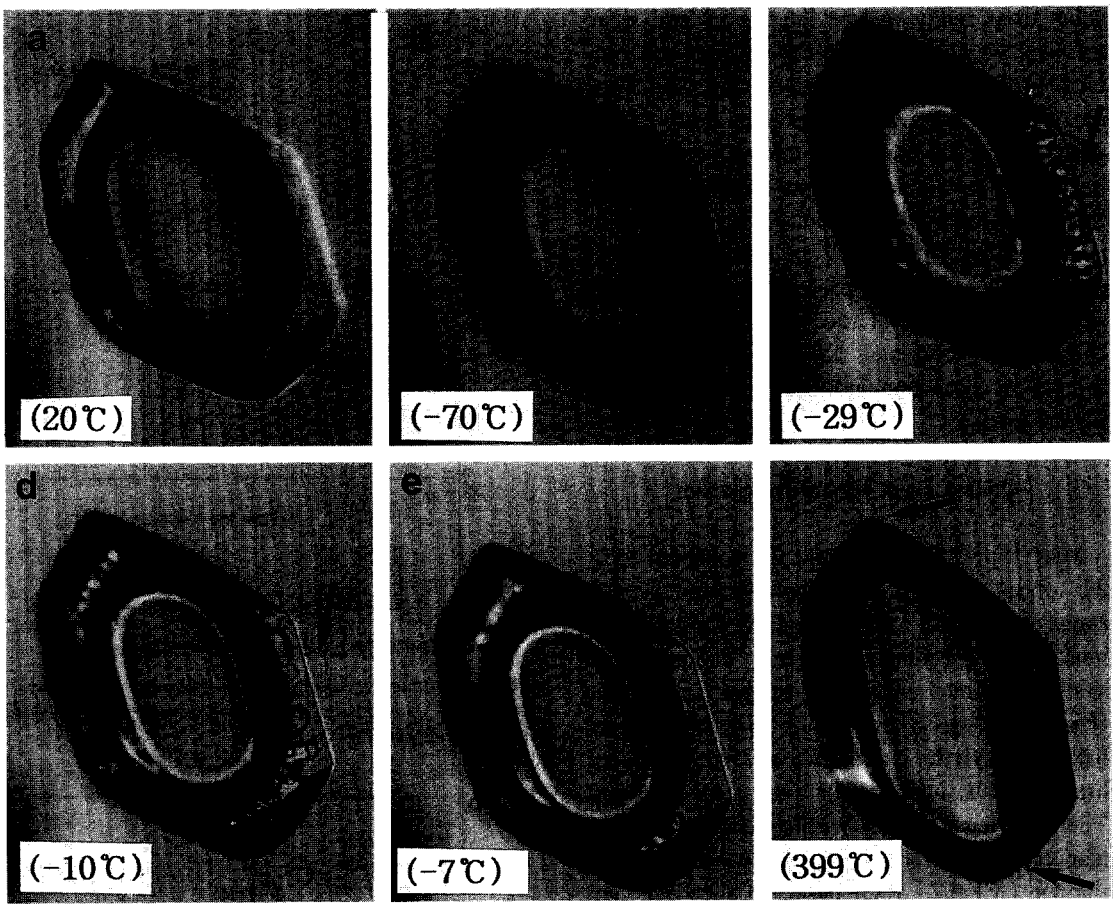

Fig. 5. Photomicrographs showing the appearance after sequential cooling and heating of a Type I inclusion. All photographs were taken at temperatures indicated in parentheses. The inclusion is 150 μm in size.

RESULTS

Type I inclusion

Initial melting of ice (eutectic temperatures) between -34 and -25℃ was observed in type I inclusions along the growth zones in euhedral quartz in miarolitic cavities, suggesting the presence of cations such as K, Na, and Ca. Fig. 5 shows the typical phase changes observed during cooling and heating experiments. When the inclusion was cooled down to -70℃ (Fig. 5b), it was completely frozen and the refractive index was changed showing a bit blurred feature. At -29℃ or below, the initial melting of ice was observed with a small amount of liquid phase at the inclusion wall (see an arrow in Fig. 5c). More liquid was formed as the temperature increased (Fig. 5d and e) and the final melting of ice occurred at -5.6℃, indicating salinity of 8.7 wt. % NaCl (Fig. 4). Most primary type I inclusions along the growth zones in euhedral quartz in miarolitic cavities showed final melting of ice at temperatures between -5.6 and 0℃, indicating salinities of 8.7 to 0 wt. % NaCl equiv. (Fig. 4).

Homogenization temperatures vary from 370 to 465℃ (Fig. 3). A histogram of homogenization temperatures of primary fluid inclusions displays a distinct cluster of data between 370 and 400℃ (Fig. 4). They have salinities between 0 and 1.6 wt. % NaCl equiv. Type I in-

clusions, upon heating, remained unchanged until the temperature approached 50℃ below the Th of the inclusions and then gradually homogenized by the vapor bubble expansion (Fig. 5a and f). No microthermometric data were obtained from type I inclusions in fissure-filling vein quartz. Because a liquid phase could not be recognized in these inclusions at room temperature, no change in the inclusions (homogenization) was apparent during heating.

Type II inclusion

Type II inclusions trapped in clear and milky quartz from hydrothermal veins associated with ore mineralization show first and final ice-melting temperatures at about -40℃ to -29℃ and between -27.4 and -1.5℃ (corresponding to salinities of 24-3 wt.% NaCl equiv.), respectively (Fig. 4). These eutectic temperatures also require the presence of additional cations besides sodium. They have the wide homogenization temperatures between 309 and 473℃ (Fig. 3). Homogenization temperatures of primary type II inclusions displays two distinct clusters of data: a group between 380 and 390℃ with salinities of 3-4 wt.% NaCl equiv., and the other group between 420-440℃ with salinities of 14-15 wt.% NaCl equiv., respectively (Fig. 4).

Type III inclusion

The different melting behaviors of halite-bearing inclusions in magmatic and hydrothermal quartz indicate that they were trapped in different regions of pressure-temperature conditions (Cline and Bodnar, 1994, Yang and Lee, 1998). Based on the homogenization behavior, type III inclusions are divided into two subtypes: Type IIIa inclusions in magmatic quartz homogenize by halite dissolution (Fig. 2c) and Type IIIb inclusions in hydrothermal quartz by vapor-bubble disappearance (Fig. 2d). Note relatively large halite crystal and a small vapor bubble of type IIIa inclusions in Fig. 2c compared to those in Fig. 2d, suggesting a different melting behavior. Type IIIa inclusions homogenized at temperatures between 305 and 359 ℃, corresponding to 38 to 43 wt.% NaCl equiv. (Fig. 3 and 4). A histogram of homogenization temperatures of primary type IIIa inclusions in magmatic quartz displays one distinct clusters of data between 310 and 330℃ of salinities of 38-40 wt. % NaCl equiv.

Type IIIb inclusions in miarolitic quartz from the granitic rocks have the homogenization temperatures of 303-376℃ with salinities of 34-38 wt. % NaCl equiv. (Fig. 3 and 4). These inclusions occur together with type I inclusions along the growth zones possibly indicating fluid immiscibility. Fig. 6 shows the melting behaviors of typical type IIIb inclusions during cooling and heating experiments. Upon heating (Fig. 6a), sylvite dissolution is the first phase at 98-139℃ followed by erythrosiderite ($K_2FeCl_5 \cdot H_2O$) dissolution at 162-250℃ (Fig. 6b). The next phase change in heating is the halite dissolution at temperatures of 230-305℃ (Fig.

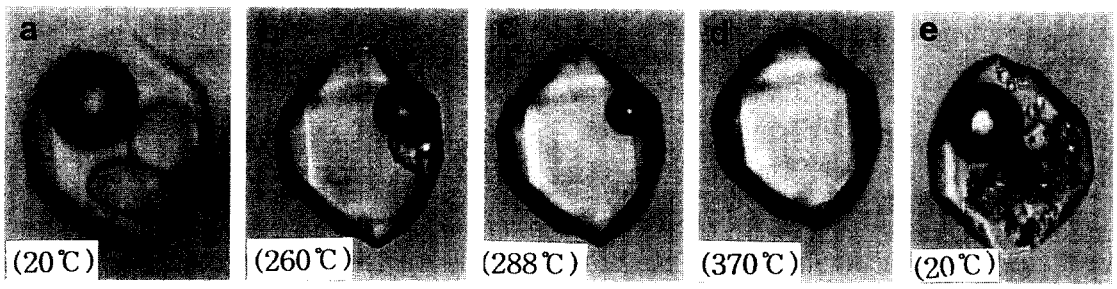

Fig. 6. Photomicrographs showing the appearance after sequential heating of a Type IIIb inclusion. All photographs were taken at temperatures indicated in parentheses. The inclusion is 120 μm in size.

6c). With the continued heating, vapor-bubble disappearance at temperatures of 303-376℃ was observed as the final phase changes (Fig. 6d). As temperature decreased again following homogenization, sylvite and erythrosiderite renucleated not as a single crystal but as aggregates of small granular grains or anhedral irregular grains (Fig. 6e). Moreover, halite sometimes renucleated not as a single cubic crystal shape (Fig. 6e). Unidentified opaque daughter minerals or a transparent crystal always persisted after the halite dissolution.

DISCUSSION AND SUMMARY

Type IIIa inclusions represent the earliest fluid based because they present only in quartz phenocrysts of granites. They homogenized by halite dissolution, as has been commonly observed in other granitic rocks of the Kyongsang basin (Yang and Bodnar, 1994; Yang, 1996a, 1996b). These fluids probably formed by direct exsolution from the crystallizing granitic magma. If they were exsolved from the crystallizing magma, they should require a considerable pressure correction for solidus temperatures (around 600℃) of granitic rocks. Assuming that the solidus and minimum trapping temperatures of a fluid are 600 and 330℃, respectively, they need about 270℃ pressure correction which corresponds to approximately 2.7 kbars. This high pressure system may have formed due to the deep crustal depth or the overpressuring accompanying progressive partitioning of aqueous fluid inside a crystallizing melt. Furthermore, this high pressure system may have generated the high salinity (38 to 43 wt% NaCl) fluid. Partitioning of chlorine between coexisting aqueous fluid and melt is a function of the system pressure (Shinohara *et al.*, 1989). High salinities in exsolving fluid from a typical calc-alkaline melt can be formed above approximately 1.3 kbars (Cline and Bodnar, 1991). As an alternative explanation for the low homogenization temperatures of type IIIa inclusions, we cannot exclude the possibility that inclusion volumes were re-equilibrated after entrapment, despite the fact that the inclusions are texturally primary and show the consistent homogenization temperature data with a small range.

Shelton *et al.* (1986) reported that the deposition of molybdenite, wolframite and scheelite occurred from the fluids with salinity of 5-25 wt. % NaCl equiv. at temperatures of 300-550℃, whereas we presents data with the Th and salinity of 309-473℃ and 3-24 wt. % NaCl equiv. with two distinct clusters at 380-390℃ and 420-440℃ (Fig. 4), which are in the comparable range of the data by Shelton *et al.*, (1986). In order to find the minimum trapping pressure of type II inclusions, data points that encompass inclusions in which total homogenization temperatures, 380 and 440℃ and salinities, 5 and 15 wt. % NaCl equiv. have been selected in the P-T space of Bodnar and Vityk (1994) (Fig. 7). These data suggest that the minimum trapping pressures of type II inclusions is 300 (point A in Fig. 7a)-500 (point B in Fig. 7b) bars. Shelton *et al.* (1986) calculated the trapping pressures of less than 100 to 300 bars, assuming that this type of fluid was generated by boiling which is not required pressure corrections. We could not obtain the evidence of boiling during the Mo-W mineralization at Sannae mine. It is equivocal that a fluid boiled at this stage and should be re-evaluated with respect to some points discussed in the following paragraph. This study favors these type II inclusions associated with ore mineralization were trapped at higher pressures than 300-500 bars.

The trapping conditions of fluid inclusions trapped in the two-phase (L+V) field can be obtained by petrographic and pressure, volume, temperature, and composition techniques (PVTX) (Bodnar and Vityk, 1994). At the Sannae mine, the petrographic evidences that saline (type IIIb) and vapor-rich inclusions (type I) coexist spatially in euhedral quartz from miarolitic cavities and phase equilibrium constraints that type IIIb inclusions homogenized by halite dis-

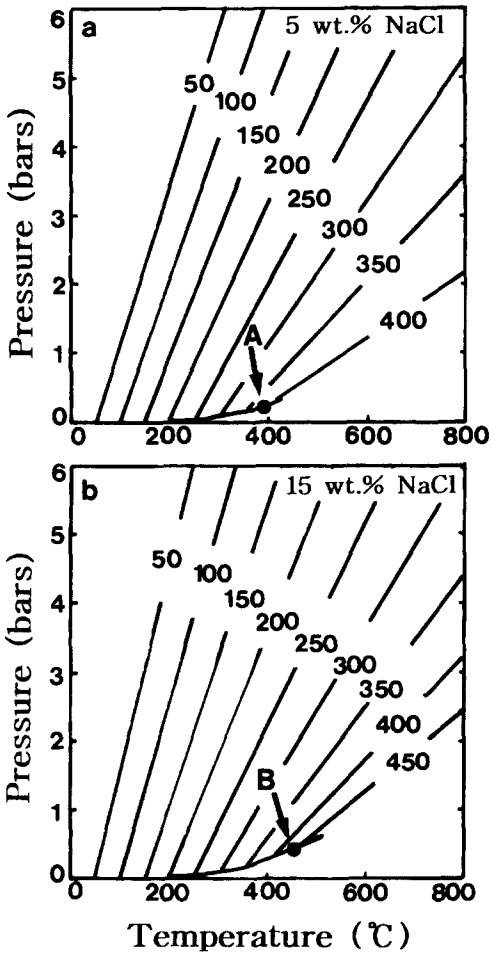

Fig. 7. Diaqrams Showing iso-Th lines for NaCl-H_2O fluids with salinities of 5 and 15 wt. % NaCl illustrating trapping conditions of type II inclusions in fissure-filling quartz veins (after Bodnar and Vityk, 1994). See the text for details.

solution are indicating coeval trapping and thus, certain fluid boiling. To confirm the fluid boiling, final homogenization temperatures of the saline inclusions and vapor-rich inclusions should be the same. However, our data show that homogenization temperatures of type I inclusions are somewhat higher than those of type IIIb inclusions (Fig. 4). This may be due to the fact that homogenization temperatures of vapor-rich inclusions is always overestimated by the small amounts of liquid along with the vapor phase (Bodnar et al., 1985). As expected, homogenization temperatures of type I inclusions in miarolitic quartz are higher than coexisting type IIIb inclusions (Fig. 4). Therefore, actual homogenization temperatures of boiling fluids during the deposition of miarolitic quartz can be reflected by type IIIb inclusions.

Within athe P-T space for NaCl-H_2O system, data points that encompass the type IIIb inclusions with the homogenization temperatures by vapor bubble disappearance and salinity of 303-376℃ and 34-38 wt. % NaCl equiv. were selected. These homogenization temperatures and salinity data are referred to vapor-pressure curves for high salinity H_2O-NaCl solutions. The intersection of the isopleth corresponding to the inclusion composition with the measured homogenization temperature in P-T space defines the pressure at the time of trapping (e.g., Yang and Lee, 1998). Halite-bearing inclusions with salinities of 34-38 wt. % NaCl and the final homogenization temperature of 303-376℃ would have been trapped at about 50 to 150 bars (Fig. 8). Based on the occurrence, the relatively low homogenization temperatures, and trapping pressure, these boiling fluids are thought to represent the late fluid to affect the Granite. The compositions, melting behaviors, and the occurrence of variable dau-

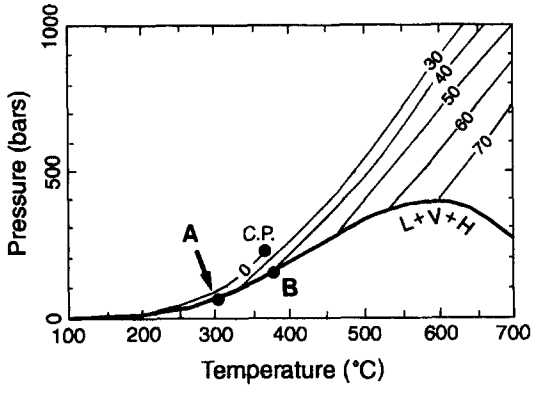

Fig. 8. Vapor-pressure curves for H_2O-NaCl solutions having salinities of 30-70 wt% NaCl (after Bodnar and Vityk, 1994). Also shown is the liquid-vapor curve for H_2O, the H_2O critical point (C.P.), and the three-phase (L+V+H) curve in the H_2O-NaCl system. See the text for details.

ghter crystals such as halite, sylvite, and erythrosiderite indicate that the fluids contained components such as KCl, $CaCl_2$, and $FeCl_2$ in addition to NaCl.

A large number of subparallel fissure-filling quartz veins associated with molybdenite-tungsten mineralization appear to be localized in small areas within the Sannae granite. Both major fault crosscutting the host granitic rocks (Fig. 1) and the ore mineralization within the sheared zone (Shelton, *et al.*, 1986) suggest the temporal and spatial relationship between Mo-W mineralization and tectonic events after the emplacement of the granite. Available radiometric ages of the host granite and the Mo-W mineralization are 75.5±1.2 Ma (Choo and Kim, 1981) and 65±3 Ma (Fletcher and Rundle, 1977), respectively, showing almost 10 Ma difference. Fluid circulation driven by magmatic heat is generally expected to occur within only a short period of time ($<10^6$ years) following the intrusion (Cathles, 1981). Therefore, we consider that the hydrothermal fluids responsible for the W-Mo vein mineralization of the Sannae mine was not from the direct exsolution of primary magmatic melt but derived from hydrothermal leaching of the elements by fluid-host rock interactions.

In conclusion, this study demonstrates that the Sannae granite was a locus for repeated fluid events including magmatic fluids during the final stage of crystallization, the convection of hydrothermal fluids causing a fluid ascending, fluid boiling, and the local W-Mo mineralization and formation of miarolitic cavities due to thermal, tectonic and compositional properties of the felsic granite.

ACKNOWLEDGMENTS

We would like to thank Professor M.E. Park for discussing of this subject and allowing to use his well-equipped fluid inclusion instruments. Many graduate students of applied geology department in Pukyong National University are greatly thanked for the help in their lab. The present study was supported by Korea Science Engineering Foundation under the program of the International cooperative research (project No. 976-0400-003-2).

REFERENCES

Bajwah, Z. U., White, A. J. R., Kwak, T. A. P. and Price, R. C., 1995, The Renison granite, Northwestern Tasmania: A petrological, geochemical and fluid inclusion study of hydrothermal alteration. Econ. Geol., 90, 1663-1675.

Bodnar, R. J. and Vityk, M. O., 1994, Interpretation of microthermometric data for H_2O-NaCl fluid inclusions: In: Vivo, B. De and Frezzotti, M. L. (eds.), Fluid Inclusions in Minerals, Methods and Applications. Virginia Polytechnic Institute and State University, VA, p. 117-130.

Bodnar, R. J., Sterner, S. M. and Hall D. L., 1989, Salty: A Fortran program to calculate compositions of fluid inclusions in the system NaCl-KCl-H_2O. Computers & Geosci., 15, 19-41.

Bodnar, R. J. and Sterner, S. M., 1987, Synthetic Fluid inclusions: in G. C. Ulmer and H. L. Barnes, eds., Hydrothermal Experimental Techniques, Wiley- Interscience, New York. 423-457.

Bodnar, R. J., Burnham, C. W. and Sterner, S. M., 1985, Synthetic fluid inclusions in natural quartz. III. Determination of phase equilibrium properties in the system H_2O-NaCl to 1000℃ and 1500 bars. Geochim. Cosmochim. Acta, 49, 1861-1873.

Cathles L. M., 1981, Fluid flow and genesis of hydrothermal ore deposits. Econ. Geol. 75th Anniv. 424-457.

Choo, S. H. and Kim, D. H., 1981, Rb/Sr age determination on Yoocheon granite, Changweon granite and Andong granite and granitic gneiss: Geosci. Mineral resources (Seoul) Rept., 12, 183-185.

Cline, J. S. and Bodnar, R. J., 1994, Direct evolution of brine from a crystallizing silicic melt at the Questa, New Mexico, Molybdenum deposit. Econ. Geol., 89, 1780-1802.

Cline, J. S. and Bodnar, R. J., 1991, Can economic porphyry copper mineralization be generated by a typical calc-alkaline melt? Jour. Geophy. Research, 96, 8113-8126.

Fletcher, C. J. N. and Rundle, C. C., 1977, Age of mineralization at Sannae and Ilkwang mines, Gyeongsang basin, Republic of Korea: Geol. Soc. Korea Jour., 13, 71-75.

Hong, S. H. and Choi, P, 1988, Geologic report of

the Yuchon sheet (1:50,000), Korea Institute od Energy and Resources.

Roedder, E., 1984, Fluid inclusions, Rev. Mineral., 12, 644p.

Shelton, K. L., So, C. S., Rye, D. M., and Park, M. E., 1986, Geologic, sulfur isotope, and fluid inclusion studies of the Sannae W-Mo mine, Republic of Korea: Comparision of sulfur isotope systematics in Korean W deposits, Econ., Geol., 81, 430-446.

Shinohara, H., Iiyama, J. T. and Matsuo, S., 1989, Partition of chlorine compounds between silicate melt and hydrothermal solutions: I. Partition of NaCl-KCl. Geochim. Cosmochim. Acta, 53, 2617-2630.

Stefanini, B. and Williams-Jones, A. E., 1996, Hydrothermal evolution in the Calabona porphyry copper system (Sardinia, Italy): the path to an uneconomic deposit, Econ. Geol., 91, 774-791.

Yang, K. and Lee, J. Y., 1998, Fluid inclusion of the Ilkwang Cu-W-bearing breccia-pipe deposit, Kyongsang Basin. Geosci. 2, 15-25.

Yang, K., 1996a, The use of fluid inclusions to constrain P-T-X conditions of formation of Eonyang amethyst. J. Petro., Soc. Korea, 5, 1-9.

Yang, K., 1996b, Fluid inclusions trapped in quartz veins and granitic rocks from Pusan-Kyeongju area. Jour. Geol. Soc. Korea, 32, 431-446.

Yang, K. and Bodnar, R. J., 1994, Magmatic-hydrothermal evolution in the bottoms of porphyry copper systems: evidence from the silicate melt and aqueous fluid inclusions in the Gyeongsang Basin, South Korea. International Geol. Rev., 36, 608-628.

(책임편집 : 문상호)
(1998년 12월 15일 접수, 1999년 2월 27일 수리)

경상분지 남동부의 산내화강암과 산내 W-MO 광상에 관한 유체포유물 연구

양경희 · 이준동

부산대학교 자연과학대학 지질학과

요 약 : 산내화강암에 영향을 준 세 종류의 유체포유물이 산내화강암과 열수석영내에 포획되어있다. 가장 초기 유체는 3상의 수용성유체포유물로서 염도(38 to 46 wt% NaCl equiv.)가 상당히 높다. 이 유체는 결정화되고 있던 용융체에서 용리되었으며, 비교적 높은 압력환경에서 포획되어진 것으로 여겨진다. 두 번째 유체는 2상의 수용성유체포유물로서 낮은 공융온도(<-40℃), 저염도 내지 중염도(3 to 24.0 wt% NaCl equiv.), 그리고 비교적 높은 균질화온도(309℃<ThL-V<473℃)로 특징지워진다. 이 유체는 300-500 bars 보다는 높은 압력에서 포획되었으며, 몰리브데나이트, 흑중석, 회중석을 함유한 광화석영맥을 침전시켰다. 마지막 유체는 고염도(34-38 wt% NaCl equiv.)와 저염도(0 to 8.7 wt%)의 유체로 비등을 한 유체로서 303-376℃, 50-150 bars에서 포획되었다. 이 비등을 한 유체는 정동내의 자형의 석영을 침전시켰으며, 상당히 복잡한 성분의 유체로서 H_2O-NaCl-KCl-$FeCl_2$계에서 형성된 유체이다. 산내화강암의 열적, 조구조적, 성분적 속성에 의해 마그마기 후기의 수용성유체의 용리부터 유체의 상승, 유체의 비등이 이루어졌으며, 이러한 왕성한 유체의 활동이 궁극적으로 산내의 W-Mo 광화대를 형성한 것이다.

핵심어 : 유체포유물, 열수석영, 용리, 수용성 유체의 비등, W-Mo 광화